Epigenetic Loss of m^{1}A RNA Demethylase ALKBH3 in Hodgkin Lymphoma Targets Collagen Conferring Poor Clinical Outcome

Rosaura Esteve-Puig,[1] Fina Climent,[2] David Piñeyro,[1,3] Eva Domingo-Domènech,[4] Veronica Davalos,[1] Maite Encuentra,[4] Anna Rea,[1] Nadia Espejo-Herrera,[2] Marta Soler,[1] Miguel Lopez,[1] Vanessa Ortiz-Barahona,[1] Gustavo Tapia,[5] Jose-Tomas Navarro[1,6], Joan Cid,[7] Lourdes Farré,[8,9] Alberto Villanueva,[8] Isolda Casanova,[1,10,11] Ramon Mangues,[1,10,11] Pablo Santamarina-Ojeda,[12] Agustín F. Fernández,[12] Mario F. Fraga,[12] Miguel Angel Piris,[3,13] Nitzan Kol,[14,15] Chen Avrahami,[14,15] Sharon Moshitch-Moshkovitz,[14,15], Gideon Rechavi[14,15], Anna Sureda[4] and Manel Esteller[1,3,16,17]

[1]Josep Carreras Leukaemia Research Institute (IJC), Badalona, Barcelona, Catalonia, Spain. [2]Department of Pathology, Hospital Universitari de Bellvitge, Universitat de Barcelona, Bellvitge Biomedical Research Institute (IDIBELL), L'Hospitalet, Barcelona, Catalonia, Spain; [3]Centro de Investigacion Biomedica en Red Cancer (CIBERONC), 28029 Madrid, Spain. [4]Clinical Hematology Department, Catalan Institute of Oncology (ICO), Hospital Duran i Reynals, L'Hospitalet, Barcelona, Catalonia, Spain. [5]Department of Pathology, Hospital Germans Trias i Pujol, Institut d'Investigació en Ciències de la Salut Germans Trias i Pujol (IGTP), Universitat Autònoma de Barcelona, Badalona, Catalonia, Spain. [6]Department of Hematology, Catalan Institute of Oncology (ICO), Hospital Universitari Germans Trias i Pujol, Universitat Autònoma de Barcelona, Badalona, Barcelona, Catalonia, Spain. [7]Apheresis & Cellular Therapy Unit, Department of Hemotherapy and Hemostasis (ICMHO), Institut d'Investigacions Biomèdiques August Pi i Sunyer (IDIBAPS), Hospital Clínic, University of Barcelona, Barcelona, Catalonia, Spain. [8]Program Against Cancer Therapeutic Resistance (ProCURE), Catalan Institute of Oncology (ICO), Bellvitge Biomedical Research Institute (IDIBELL), L'Hospitalet de Llobregat, Barcelona, Catalonia Spain. [9]Laboratory of Experimental Pathology (LAPEX), Gonçalo Moniz Research Center, Oswaldo Cruz Foundation (CPQGM/FIOCRUZ), Salvador, Bahia Brazil. [10]CIBER de Bioingeniería Biomateriales y Nanomedicina (CIBER-BBN) 28029 Madrid, Spain. [11]Biomedical Research Institute Sant Pau (IIB-Sant Pau), Hospital de la Santa Creu i Sant Pau 08041 Barcelona, Catalonia, Spain. [12]Nanomaterials and Nanotechnology Research Center (CINN-CSIC), Health Research Institute of Asturias (ISPA), Institute of Oncology of Asturias (IUOPA) and Department of Organisms and Systems Biology (B.O.S), University of Oviedo, Oviedo, Spain. [13]Service of Pathology, Fundación Jiménez Díaz University Hospital, Madrid, Spain. [14]Cancer Research Center and Wohl Institute for Translational Medicine, Chaim Sheba Medical Center, Tel-Hashomer, Israel; [15]Department of Human Genetics and Biochemistry, Sackler Faculty of Medicine, Tel Aviv University, Tel Aviv, Israel. [16]Institucio Catalana de Recerca i Estudis Avançats (ICREA), Barcelona, Catalonia, Spain. [17]Physiological Sciences Department, School of Medicine and Health Sciences, University of Barcelona (UB), Barcelona, Catalonia, Spain.

The dysregulation of RNA and protein levels, in comparison to the counterpart normal tissues, is a constant molecular feature of all human malignancies. Many causes can be invoked as culprits of the altered transcriptome and proteome of cancer cells, but recently the emergence of disrupted chemical modifications of the RNA molecule that can affect its stability, targeting or translation is gaining momentum. In this regard, the emergence of a so termed altered epitranscriptome is starting to be described in tumorigenesis,[1,2] including malignant hematopoiesis.[3] More than 100 distinctly modified nucleotides have been described in RNA molecules.[4,5] Although some of these have also been described in DNA, such as cytosine methylation, DNA has a smaller repertoire of modified nucleotides, whereas RNA molecules can show a more diverse spectrum of modifications that includes, among others, pseudouridine or queuosine. However, the most abundant modification of RNA is the methylation of adenosine (A) in the form of m^6A and to a lesser extent of m^1A. m^6A is the most common internal modification of mRNA affecting various facets of RNA metabolism,[5,6] but it is also relevant to microRNAs, controlling their maturation and expression levels, such as it has been described for the tumor-suppressor miRNA let-7.[7] The other methylated adenosine present in RNA, m^1A, is typically found in abundant ncRNAs, but it is also observed around the start codon upstream of the first splice site and in the 5′ Untranslated Regions (UTRs) of mRNAs.[8-10] The m^1A location is opposed to m^6A that is enriched in 3′ UTRs and near stop codons.[11,12]

The discovery of an m^6A eraser, FTO,[13] provided the first evidence of reversible posttranscriptional modifications in mRNAs and further fire up the interest in the epitranscriptome and its possible impact in cancer biology. Since then, complex pathways of highly regulated enzymes that add (writers) or remove (erasers) the RNA modifications marks have been dissected in the physiological level, but little is still know about their possible alterations in the cancer arena. Focusing on the methylation of the adenosine, the most prevalent type of RNA modification, and knowing that promoter CpG island hypermethylation-associated transcriptional silencing is a common mechanism of gene inactivation in cancer cells,[14,15] we interrogated the presence of this type of epigenetic inactivation in the genes encoding the writers and erasers of the m^6A and m^1A marks. Thus, herein we have investigated cancer-specific DNA methylation changes in the 5`-end promoter regions of the METTL3 and METTL14 core subunits of the m^6A writer complex; the m6A erasers ALKBH5 and FTO; the m1A writers TRMT6, TRMT61A, TRMT10C and TRMT61B; and the m1A eraser ALKBH3.[5] To uncover candidate epigenetic changes in these enzymes, we first data-mined a collection of close to 1,000 human cancer cell lines in which we have characterized the DNA methylation profiles.[16] The promoter-associated CpG islands of METTL3, METTL14, ALKBH5, FTO, TRMT6, TRMT61A, TRMT10C and TRMT61B were unmethylated in all the assessed cancer cell lines (**Supplemental Dataset S1**). However,

the ALKBH3 promoter CpG island was commonly methylated in lymphoma cell lines (35%, 23 of 66) among different cancer cell lines types (**Figure 1A and Supplemental Dataset S1**). The second tumor type with the highest percentage of ALKBH3 hypermethylation was breast cancer (10.20%, 5 of 49), where this epigenetic alteration has recently been described.[17] Although ALKBH3 has been reported to be upregulated in head and neck cancer,[18] data-mining of the available transcriptional patterns in the studied cancer cell line set[16] showed that ALKBH3 hypermethylation was associated with mRNA downregulation (**Figure 1B**). This genomic locus was found unmethylated in all the different normal tissue samples analyzed from the TCGA dataset (n=730) (**Supplemental Dataset S2**). Further detailed *in silico* analyses of the hematological malignancies according to their subtype identified that ALKBH3 promoter CpG island hypermethylation was most frequent in Hodgkin lymphoma cell lines (44%, 4 of 9), followed by Burkitt lymphoma (38%, 5 of 13), other Non-Hodgkin lymphoma cell lines (37%, 12 of 32) and anaplastic large cell lymphoma (33%, 1 of 3). (**Figure 1C**). Data-mining of the available microarray expression results[16] demonstrated that ALKBH3 hypermethylation was linked to transcript downregulation in the cell lines derived from hematological malignancies (**Figure 1D**). Further *in silico* analyses showed that the 5'-end of of ALKBH3 was unmethylated in all the tested samples of Peripheral Blood Mononuclear Cells (PBMCs), naive B-lymphocytes and naive T-lymphocytes obtained from healthy donors (**Supplemental Dataset S3**). Thus, the cancer-specific DNA methylation event at the ALKBH3 promoter became our focus of interest and was herein further studied in the context of Hodgkin lymphoma, the lymphoma type exhibiting the highest hypermethylation frequency.

Having found the ALKBH3 CpG island methylation patterns shown above, we assessed in detail the possible association of the hypermethylation event with the loss of ALKBH3 gene expression at the RNA and protein levels. We performed bisulfite genomic sequencing of multiple clones in the Hodgkin lymphoma cell lines KM-H2, L540, HS445 and HD-MY-Z using primers that encompassed the transcription start site-linked CpG island (**Supplementary Methods**). We observed that the 5'-end CpG island of ALKBH3 in the L540 and KMH2 cell lines was hypermethylated (**Figure 1E**), whereas the HD-MY-Z and HS445 cells were unmethylated at these sites (**Figure 1E**). Naive B-cells were also found unmethylated (**Figure 1E**). These data corroborated the DNA methylation profiles obtained by the DNA methylation microarray platform (**Figure 1F**). The methylated ALKBH3 cell lines KM-2 and L540 did not express the ALKBH3 RNA transcript and protein, as determined by quantitative reverse transcription PCR and western blot, respectively (**Figure 1G**). Expression of ALKBH3 RNA and protein was found in the unmethylated cell lines HD-MY-Z and HS445 (**Figure 1G**). Treatment of the ALKBH3-hypermethylated cell lines with the DNA demethylating agent 5'-aza-2'-deoxycytidine restored ALKBH3 RNA and protein expression

(**Figure 1H**). The association between ALKBH3 promoter hypermethylation and gene silencing was further validated in two additional Hodgkin cell lines not included in our original screening, SUP-HD1 and HS611-T (**Supplemental Figure 1**). Overall, these results indicate the presence of cancer-specific promoter CpG island hypermethylation-associated loss of ALKBH3 gene expression in Hodgkin lymphoma cells. DNA methylation-associated silencing of ALKBH3 was also validated in thirteen cell lines derived from Burkitt lymphoma and other Non-Hodgkin lymphomas (**Supplemental Figure 2**).

Once we had shown the presence of ALKBH3 CpG island hypermethylation-linked transcriptional inactivation in human Hodgkin lymphoma cell lines, we then wondered about the molecular targets of ALKBH3 loss in these cells. Beyond its role in DNA repair,[19-21] ALKBH3 exhibits an RNA demethylase activity for m^1A mRNA.[9] Thus, the epigenetic inactivation of ALKBH3 in Hodgkin lymphoma cells hinders a downstream m^1A RNA demethylating event and this can contribute to the biology of these malignancies. To prove this idea, we performed RNA high-throughput sequencing using an m^1A antibody to enrich m^1A-modified mRNA fragments[8] in HD-MY-Z cells, unmethylated at the ALKBH3 promoter CpG island (**Figure 1E and 1F**) and expressing the transcript and protein (**Figure 1G**), transfected with a doxycycline-inducible short harpin RNA (shRNA) against ALKBH3 (**Figure 2A**). Read mapping statistics from the m^1A-sequencing samples are shown in **Supplemental Table 1**. The obtained raw data have been deposited at the SRA BioProject PRJNA602695 https://www.ncbi.nlm.nih.gov/bioproject/PRJNA602695

Upon efficient shRNA-mediated depletion of ALKBH3 in the HDMYZ cells (**Figure 2A and Supplemental Figure 3**), our epitranscriptomic approach identified that, whereas 2,511 m^1A peaks (corresponding to 1,522 transcripts) were unchanged in both conditions (**Supplemental Table 2**), the shRNA-mediated depletion of ALKBH3 in HD-MY-Z cells caused a change of 165 m^1A peaks (corresponding to 147 transcripts) (**Supplemental Table 3**). Most important, the induced downregulation of ALKBH3 caused a gain of m^1A, being observed in 159 m^1A sites (96% of the total 165 sites with distinct m^1A content) corresponding to 141 transcripts (**Supplemental Table 3**), a finding that it is consistent with the described role of ALKBH3 as an m^1A RNA demethylase.[9] The most frequent location of the differential m^1A peaks was the 5′-untranslated region (5′ UTR) of the transcripts (**Figure 2B**), in agreement with previous reports for this epitranscriptomic mark,[8,9,22] although they were also observed in other transcript regions such as exons, 3'-UTR and introns. To better characterize the identified set of 147 genes with significantly distinct m^1A content upon ALKBH3 depletion, we performed a gene functional annotation by gene set enrichment analysis (GSEA) using Gene Ontology (GO signature) collections. We observed an overrepresentation of GO biological processes, molecular function, cellular component and reactome pathways related to cell migration (such as "locomotion" and "cell motility"), the

cytoskeleton (such as “cytoskeleton organization” and “actin filament based process”) and the microenvironment (such as “extracellular matrix structural component”, “extracellular matrix organization” and collagen formation, degradation and trimerization) (**Figure 2C and Supplemental Figure 4**). These processes are highly relevant in Hodgkin lymphoma were the malignant cells are surrounded by a large tumor microenvironment that exerts a critical role in the disease[23] and the cytoskeleton, through association with extracellular connective tissues, acts as a “guardian” for tissue stabilization and the prevention of cell migration. In this regard, the two transcripts with the highest number of gained m^1A peaks upon ALKBH3 depletion corresponded to two collagens, type I alpha 2 (COL1A2) and type I alpha 1 (COL1A1) (**Supplementary Table 4**), critical noncellular components of the Hodgkin lymphoma microenvironment.[24,25] Genome browser screenshots for differential m^1A peaks in COL1A2 and COL1A1 are shown in **Supplemental Figure 5**. Presence of m^1A in 5′UTRs correlates with increased protein expression,[8,9] and we indeed observed that the shRNA-mediated depletion of ALKBH3 in HD-MY-Z cells induced high protein expression levels of both collagens (**Figure 2D**). We also performed the reverse experiment, in which we restored ALKBH3 expression by transduction in the hypermethylated/silenced cell line L540 (**Supplemental Figure 6**). Herein, we found the opposite scenario compared to the shRNA model (**Figure 2D**): the recovery of ALKBH3 expression reduced m^1A content in the COL1A2 mRNA and decreased COL1A2 protein levels (**Supplemental Figure 6**). The link between ALKBH3 epigenetic silencing and collagen expression was further reinforced by showing how restoration of ALKBH3 expression in hypermethylated KM-H2 and L540 cells upon the use of the DNA methylating agent, decreased COL1A2 levels (**Supplemental Figure 7**).

To further improve the real representation of the disease beyond the limitations of established cell lines, we studied the relevance of ALKBH3 aberrant CpG island methylation also in human primary Hodgkin lymphomas. To achieve this goal, we determined the ALKBH3 promoter methylation status by bisulfite-coupled pyrosequencing (**Supplementary Methods**) in a collection of eighty well characterized primary Hodgkin lymphoma cases whose clinicopathological features are shown in **Supplemental Table 5**. We detected ALKBH3 promoter hypermethylation in 18% (14 of 80) of the primary Hodgkin lymphoma cases. The presence of ALKBH3 aberrant methylation was not associated with any of the studied clinicopathological parameters (**Supplemental Table 5**). We also analyzed ALKBH3 expression by western-blot in four samples of the studied primary Hodgkin lymphoma cases, observing that ALKBH3 CpG island hypermethylation was associated with protein loss (**Supplemental Figure 8**). Importantly, ALKBH3 epigenetic silencing was also associated COL1A2 and COL1A1 overexpression, whereas an unmethylated ALKBH3 CpG island was linked to the absence of collagen expression (**Supplemental Figure 8**), mimicking the results found in the cell line models (**Figure 2D**). Most importantly, we wondered whether

ALKBH3 hypermethylation also conferred any clinical outcome value. We observed that ALKBH3 hypermethylation was associated with shorter Overall Survival (OS) (log-rank; P = 0.010; HR = 4.231, 95% CI= 1.290 - 13.872) (**Figure 2E**) in the studied Hodgkin lymphoma cohort. The multivariate analysis showed that ALKBH3 promoter hypermethylation demonstrated to be an independent prognostic factor for reduced OS (HR = 4.752, 95% CI = 1.277 – 17.683, p = 0.020) (**Figure 2F**).

Overall, the described research provides an illustrative example that aberrations of the so called epitranscriptome occur in human lymphomas, herein, shown by the epigenetic silencing of the m^1A RNA demethylase ALKBH3 in Hodgkin lymphoma. The epigenetic event we describe shifts the m^1A targeting of migration and cytoskeleton related genes, and provides an independent biomarker of poor overall survival in this otherwise good prognosis disease.

REFERENCES

1. Esteller M, Pandolfi PP. The Epitranscriptome of Noncoding RNAs in Cancer. *Cancer Discov.* 2017;7(4):359-368.

2. Lian H, Wang QH, Zhu CB, Ma J, Jin WL. Deciphering the Epitranscriptome in Cancer. *Trends Cancer.* 2018;4(3):207-221.

3. Vu LP, Cheng Y, Kharas MG. The Biology of m6A RNA Methylation in Normal and Malignant Hematopoiesis. *Cancer Discov*. 2019;9(1):25-33.

4. Gilbert WV, Bell TA, Schaening C. Messenger RNA modifications: Form, distribution, and function. *Science*. 2016;352(6292):1408–1412.

5. Davalos V, Blanco S, Esteller M. SnapShot: Messenger RNA Modifications. *Cell.* 2018;174(2):498-498.e1.

6. Fu Y, Dominissini D, Rechavi G, He C. Gene expression regulation mediated through reversible m6A RNA methylation. *Nat Rev Genet.* 2014;15(5):293-306.

7. Alarcón CR, Lee H, Goodarzi H, Halberg N, Tavazoie SF. N6-methyladenosine marks primary microRNAs for processing. *Nature*. 2015;519(7544):482–485.

8. Dominissini D, Nachtergaele S, Moshitch-Moshkovitz S, et al. The dynamic N(1)-methyladenosine methylome in eukaryotic messenger RNA. *Nature*. 2016;530(7591):441–446.

9. Li X, Xiong X, Wang K, Wang L, et al. Transcriptome wide mapping reveals reversible and dynamic N(1)-methyladenosine methylome. *Nat Chem Biol*. 2016;12(5):311–316.

10. Zhou H, Rauch S, Dai Q, et al. Evolution of a reverse transcriptase to map N1-methyladenosine in human messenger RNA. *Nat Methods.* 2019;16(12):1281-1288.

11. Dominissini D, Moshitch-Moshkovitz S, Schwartz S, et al. Topology of the human and mouse m6A RNA methylomes revealed by m6A-seq. *Nature*. 2012;485(7397):201-206.

12. Meyer KD, Saletore Y, Zumbo P, Elemento O, Mason CE, Jaffrey SR. Comprehensive analysis of mRNA methylation reveals enrichment in 3′ UTRs and near stop codons. *Cell*. 2012;149(7):1635–1646.

13. Jia G, Fu Y, Zhao X, Dai Q, et al. N6-methyladenosine in nuclear RNA is a major substrate of the obesity-associated FTO. *Nat Chem Biol*. 2011;7(12):885-887.

14. Baylin SB, Jones PA. Epigenetic Determinants of Cancer. *Cold Spring Harb Perspect Biol*. 2016;8(9).

15. Berdasco M, Esteller M. Clinical epigenetics: seizing opportunities for translation. *Nat Rev Genet.* 2019;20(2):109-127.

16. Iorio F, Knijnenburg TA, Vis DJ, et al. A Landscape of Pharmacogenomic Interactions in Cancer. *Cell*. 2016;166(3):740-754.

17. Stefansson OA, Hermanowicz S, van der Horst J, et al. CpG promoter methylation of the ALKBH3 alkylation repair gene in breast cancer. *BMC Cancer.* 2017;17(1):469.

18. Pilžys T, Marcinkowski M, Kukwa W, et al. ALKBH overexpression in head and neck cancer: potential target for novel anticancer therapy. *Sci Rep.* 2019;9(1):13249.

19. Ringvoll J, Nordstrand LM, Vågbø CB, et al. Repair deficient mice reveal mABH2 as the primary oxidative demethylase for repairing 1meA and 3meC lesions in DNA. *EMBO J.* 2006;25(10):2189-2198.

20. Ringvoll J, Moen MN, Nordstrand LM, et al. AlkB homologue 2-mediated repair of ethenoadenine lesions in mammalian DNA. *Cancer Res.* 2008;68(11):4142-4149.

21. Calvo JA, Meira LB, Lee CY, et al. DNA repair is indispensable for survival after acute inflammation. *J Clin Invest*. 2012;122:2680-2689.

22. Li X, Xiong X, Zhang M, et al. Base-Resolution Mapping Reveals Distinct m1A Methylome in Nuclear- and Mitochondrial-Encoded Transcripts. *Mol Cell.* 2017;68(5):993-1005.

23. Liu Y, Sattarzadeh A, Diepstra A, Visser L, van den Berg A. The microenvironment in classical Hodgkin lymphoma: an actively shaped and essential tumor component. *Semin Cancer Biol*. 2014;24:15-22.

24. Jaspars LH, Bloemena E, Bonnet P, Van der Valk P, Meijer CJ. Distribution of extracellular matrix components and their receptors in human lymphoid tissue and B-cell non-Hodgkin lymphomas. *Histopathology*. 1995;26(2):113-121.

25. Cader FZ, Vockerodt M, Bose S, et al. The EBV oncogene LMP1 protects lymphoma cells from cell death through the collagen-mediated activation of DDR1. *Blood.* 2013;122(26):4237-4245.

Figure Legends

Figure 1. ALKBH3 promoter CpG island hypermethylation and transcriptional silencing in Hodgkin lymphoma cells. (**A**) Percentage of ALKBH3 methylation in the Sanger set of cancer cell lines according to tumor type. Number of cell lines studied for each tumor type are shown on top of each column. (**B**) ALKBH3 hypermethylation is associated with loss of the mRNA in cell lines from the Sanger panel (n=957). (**C**) Percentage of ALKBH3 methylation in the Sanger set of cell lines derived from hematological malignancies according to subtype. Number of cell lines studied for each tumor type are shown on top of each column. (**D**) ALKBH3 methylation is associated with loss of the transcript in the Sanger set of cell lines derived from hematological malignancies (n=162). (**E**) Bisulfite genomic sequencing of the ALKBH3 promoter CpG island in Hodgkin lymphoma cell lines and naive B-cells from healthy donors. CpGs are represented as short vertical lines; the transcription start site (TSS) is represented as a black arrow. Single clones are shown for each sample. Presence of an methylated or unmethylated cytosine is indicated by a black or white square, respectively. (**F**) DNA methylation profile of the ALKBH3 promoter CpG island analyzed using the 450K DNA methylation microarray. Single CpG methylation levels (0 – 1) are shown. Red, methylated; green, unmethylated. Data from the four studied Hodgkin lymphoma cell lines. (**G**) Expression levels of ALKBH3 in Hodgkin lymphoma cell lines assessed by quantitative reverse transcription PCR (data shown represent mean ± SD of biological triplicates) (left) and western blot (right). (**H**) Expression of the ALKBH3 RNA transcript (data shown represent the mean ± SD of biological triplicates) and protein was recovered in the ALKBH3 hypermethylated and silenced KM-H2 and L540 cells upon use of the DNA demethylating agent 5-aza-2'-deoxycytidine (AZA). *p<0.05, **p<0.01, ***p<0.001.

Figure 2. ALKBH3 loss induces a gain of m^1A in the transcriptome of Hodgkin lymphoma cells and is associated with poor clinical outcome. (**A**) Western-blot validation of the efficient shRNA-mediated depletion of ALKBH3 in HD-MY-Z cells upon the addition of doxycycline and workflow of the RNA high-throughput sequencing using an m^1A antibody to enrich m1A-modified mRNA fragments analysis developed to detect changes in m^1A peaks upon ALKBH3 depletion in HD-MY-Z cells. (**B**) Distribution of RNA location sites for the m^1A peaks undergoing changes in upon ALKBH3 depletion in HD-MY-Z cells. (**C**) Gene ontology analysis (GO) of the genes with differential m^1A content in HD-MY-Z cells upon ALKBH3 depletion (hypergeometric test with a FDR adjusted p-value < 0.05). (**D**) Western-blot of COL1A2 and COL1A1 protein levels upon shRNA-mediated depletion of ALKBH3 in HD-MY-Z cells. (**E**) Kaplan-Meier analysis of overall survival (OS) in primary Hodgkin lymphomas according to ALKBH3 methylation status determined by

pyrosequencing. The p-value corresponds to the log-rank test. Results of the univariate Cox regression analysis are represented by the hazard ratio (HR) and 95% confidence interval (CI). (**F**) Multivariate Cox regression analysis of OS, represented by a forest plot, considering the clinical characteristics of the cohort of primary Hodgkin lymphoma patients. ALKBH3 promoter hypermethylation is an independent prognostic factor for OS. Values of $p < 0.05$ were considered statistically significant. *p<0.05.

Acknowledgments

We thank CERCA Programme/Generalitat de Catalunya for institutional support. This work was supported by the Health Department PERIS-project no. SLT/002/16/00374 and AGAUR-projects no. 2017SGR1080 of the Catalan Government (Generalitat de Catalunya); Ministerio de Ciencia e Innovación (MCI), Agencia Estatal de Investigación (AEI) and European Regional Development Fund (ERDF) project no. RTI2018-094049-B-I00; the Cellex Foundation; and “la Caixa” Banking Foundation (LCF/PR/GN18/51140001). P.S.O. is a fellow of the Severo Ochoa Program (Bp17-165). V.D. is supported by the Spanish Association Against Cancer (AECC).

Authorship

Contribution: R.E.P. and M.Es. conceived and designed the study; R.E.P., A.R., M.S., M.L., V.O.-B., P.S.O., A.F.F. and M.F. performed molecular analyses; D.P. analyzed multimomics data; F.C, E.D.D., V.D, M.En., N.E.H., G.T., J.-T.N., J.C. and A.S. provided primary samples and analyzed clinical data; L.F., A.V., I.C., R.M. and M.A.P. provided and studied cellular models; N.K., C.A., S.M.M. and G.R. performed the RNA high-throughput sequencing using the m^1A antibody. R.E.P. and M.Es. wrote the manuscript with contributions and approval from all authors.

Conflict-of-interest disclosure: ME is a consultant of Ferrer International and Quimatryx. The remaining authors declare that they have no conflict of interest.

Data sharing: Raw data have been deposited at the SRA BioProject PRJNA602695 https://www.ncbi.nlm.nih.gov/bioproject/PRJNA602695

Correspondence: Anna Sureda, Clinical Hematology Department, Catalan Institute of Oncology (ICO), Hospital Duran i Reynals, Av. Gran Via de L'Hospitalet 199–203, 08909 L’Hospitalet, Barcelona, Catalonia, Spain, e-mail: asureda@iconcologia.net ; or Manel Esteller, Josep Carreras Leukaemia Research Institute (IJC), Carretera de Can Ruti, Camí de les Escoles s/n, 08916 Badalona, Barcelona, Catalonia, Spain, e-mail: mesteller@carrerasresearch.org

Figure 1

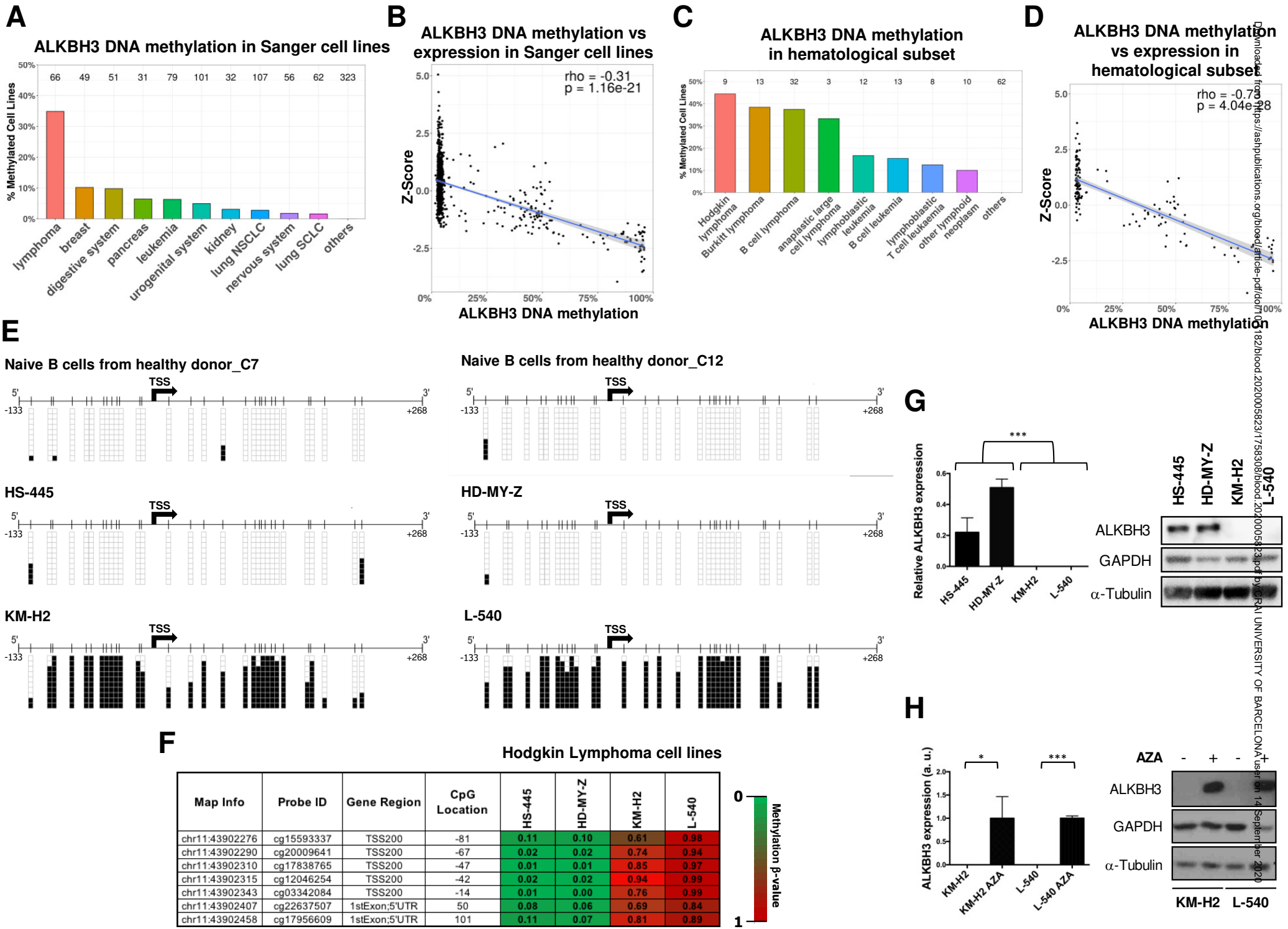

F

Hodgkin Lymphoma cell lines

Map Info	Probe ID	Gene Region	CpG Location	HS-445	HD-MY-Z	KM-H2	L-540
chr11:43902276	cg15593337	TSS200	-81	0.11	0.10	0.61	0.98
chr11:43902290	cg20009641	TSS200	-67	0.02	0.02	0.74	0.94
chr11:43902310	cg17838765	TSS200	-47	0.01	0.01	0.85	0.97
chr11:43902315	cg12046254	TSS200	-42	0.02	0.02	0.94	0.99
chr11:43902343	cg03342084	TSS200	-14	0.01	0.00	0.76	0.99
chr11:43902407	cg22637507	1stExon;5'UTR	50	0.08	0.06	0.69	0.84
chr11:43902458	cg17956609	1stExon;5'UTR	101	0.11	0.07	0.81	0.89

0 — Methylation β-value — 1

Figure 2